Physics-informed neural networks for modeling hysteretic behavior in magnetorheological dampers

Yuandi Wu[a], Brett Sicard[a], Patrick Kosierb[a], Raveen Appuhamy[a], Alex McCafferty-Leroux[a], and S. Andrew Gadsden[a]

[a]Department of Mechanical Engineering, McMaster University, Hamilton, Ontario, Canada

ABSTRACT

In this article, the power of physics-informed neural networks is employed to address the issue of model identification for complex physical systems, focusing on the application of a magnetorheological (MR) damper setup. The research leverages the Bouc-Wen hysteresis model, a well-established representation of nonlinear behavior in MR dampers, to inform the training process of a series of cascaded neural networks. The core objective of this research is to develop a surrogate model capable of accurately predicting the dynamic behavior of MR dampers under various operational conditions. Traditionally, MR dampers pose significant modelling challenges due to their nonlinear and hysteresis-rich characteristics. The approach explored in this article combines physics-based insights with the capabilities of neural networks to resolve the complexity associated with the modelling process. The methodology involves the formulation of a physics-informed loss function, which embeds the Bouc-Wen hysteresis model's governing equations into the training process of the neural networks. This fusion of physical principles and machine learning enables the networks to inherently capture the underlying physics, resulting in a more accurate and interpretable surrogate model. Through experimentation, the effectiveness of the physics-informed neural network approach in surrogate modeling for MR dampers is demonstrated. The model developed exhibits decent predictive performance across a range of input parameters and excitation conditions, offering a promising alternative to conventional black-box machine learning and physics-based methods. Furthermore, this research showcases the potential for physics-informed machine learning in modelling complex physical systems, offering a perspective on the utility of this approach in other engineering and scientific domains. The application of this methodology further facilitates improved control and optimization strategies in various engineering applications.

Keywords: Machine Learning, Physics-Informed Machine Learning, Physics-Informed Neural Networks, Surrogate Modelling, Magnetorheological Damper

1. INTRODUCTION

Machine learning (ML) has drastically enhanced automation in various industries by enabling the development of algorithms capable of learning from data and making predictions or decisions with enhanced autonomy (1). Deep learning, a subset of ML, has garnered significant attention due to its ability to automatically learn hierarchical representations of data through neural networks (NN) (2; 3; 4). Unlike traditional ML methods that rely on handcrafted features, deep learning algorithms can learn complex features directly from raw data, leading to superior performance in tasks such as image recognition (5; 6; 7) and natural language processing (8; 9). However, the success of deep learning comes with significant requirements with respects to data, often necessitating large volumes of labeled data for training. This reliance on extensive datasets can pose challenges in practical applications, especially in domains where labeled data is scarce or expensive to obtain (10; 11).

There has been a growing recognition of the challenges posed by the significant data requirements of deep learning models. One promising approach to address these challenges is through the use of physics-informed neural networks (PINNs), as numerous authors have already noted (12; 13; 14; 15). These networks leverage known physical principles or constraints to guide their learning process, reducing the requirements of quantity

Further author information: (Send correspondence to Yuandi Wu)
Yuandi Wu: E-mail: wuy187@mcmaster.ca, Telephone: 1 (905) 525 9140 ext. 21121

Artificial Intelligence and Machine Learning for Multi-Domain Operations Applications VI, edited by Peter J. Schwartz, Benjamin Jensen, Myron E. Hohil, Proc. of SPIE Vol. 13051, 130511G · © 2024 SPIE · 0277-786X · doi: 10.1117/12.3012777

of labeled data (13; 16). Additionally, they offer the benefit of enhanced interpretability in integrating physical principles with training data, enabling the developed algorithm to learn and compensate for uncertainties inherent in the physical models. Through combining domain knowledge with data-driven techniques, physics-informed ML aims to develop models that perform well on tasks, and also adhere to known physical laws or principles (16; 17). This is especially pertinent considering conventional ML algorithms operate in a purely data-driven manner, often overlooking available prior knowledge. Through striking a balance between physical principles and empirical data, physics-informed ML offers a promising framework for addressing the challenges posed by imperfect understanding of complex systems.

Surrogate modeling, a technique used to approximate complex systems with more simple and computationally efficient models, finds significant utility in applications requiring interpretable and transparent artificial intelligence models (18). Physics-informed ML offers a robust framework for enhanced interpretability and reliability by merging domain expertise with data-driven techniques (19). This integration of physics and ML holds promise across various domains, including engineering design optimization and simulation (19; 20; 21; 22). In the context of magnetorehological (MR) dampers, which are semi-active devices used for vibration control in engineering applications, modeling their complex nonlinear behavior poses a significant challenge. MR dampers exhibit hysteretic effects between force and velocity, making them difficult to accurately characterize using traditional modeling approaches (23; 24). While several modeling techniques, such as the modified Bouc-Wen model, have been proposed to capture the hysteretic behavior of MR dampers, these models are often either too complex or lack accuracy, limiting their practical utility (24).

In this study, a PINN is used to construct a surrogate model to approximate the hysteretic behavior of MR dampers. Surrogate modeling offers a computationally efficient alternative to traditional numerical simulations, making it well-suited for real-time control applications (25). Leveraging physics-informed ML techniques, the surrogate model aims to balance between computational efficiency and accuracy, with the objective of providing a practical solution for modeling the complex hysteretic behavior of MR dampers.

The document is structured as follows: Section 2 provides background information on MR dampers, including popular numerical modeling approaches such as the Bouc-Wen model, which details the physics of the system. Section 3 discusses PINNs, their development, working principles, and their applications. Section 4 introduces the proposed approach and its derivation based on the Bouc-Wen Model. Section 5 presents the results of the developed surrogate model and provides a discussion of its derivation. Finally, Section 6 concludes the article.

2. MODELLING A MAGNETORHEOLOGICAL DAMPER

MR dampers play a crucial role in various engineering applications where precise and rapid control over damping characteristics is essential. One prominent application is in vehicle suspension systems, where MR dampers offer adaptability to changing road conditions, providing both comfort and stability to occupants (26; 27; 28; 29). In civil engineering, MR dampers are utilised in seismic isolation systems to mitigate the effects of earthquakes on structures, safeguarding infrastructure and ensuring occupant safety (30; 31; 32). Accurate modeling of MR dampers is paramount due to their dynamic nature. A comprehensive understanding of their behavior enables engineers to optimize performance, predict system response, and develop robust control strategies. Mathematical modeling of MR dampers involves capturing the complex interplay between magnetic field strength, fluid viscosity, and mechanical motion. This requires models incorporating nonlinear dynamics to accurately simulate the damping characteristics under varying conditions (33). Efforts to physically model MR dampers have been the focus of extensive research. Various approaches have been explored to accurately capture the complex behavior of MR dampers, including mathematical modeling, system identification, and experimental validation (24; 33; 34; 35). These attempts aim to develop comprehensive models that can effectively predict the dynamic response of MR dampers under diverse operating conditions. Combining theoretical formulations with empirical data, researchers seek to enhance the understanding and predictive capabilities of physical models.

Several numerical models have been devised to simulate the behavior of MR dampers, each offering a unique perspective on the complex dynamics of these devices. Notable among these models in use in the industry are the Bingham (36), viscoelastic-plastic (37), hydromechanical (38), Maxwell (39), Dahl (40), and LuGre models (41). These formulations incorporate diverse mathematical frameworks to represent the rheological and mechanical characteristics of MR dampers, considering factors such as yield stress, viscosity, elasticity, plasticity, and sliding friction. Among the diverse numerical models applied to simulate the behavior of MR dampers, the Bouc-Wen model has emerged as a prominent approach (24; 33). The Bouc-Wen model is characterized as a parametric model. It is structured to represent the mechanical system through an arrangement of ideal spring and ideal passive dampers, and illustrated in Figure 1. This model is represented by a mathematical function, as will be detailed further in this section, necessitating the identification of coefficients or parameters. This identification process typically entails the utilisation of optimization techniques (42; 43). Given its phenomenological nature, the Bouc-Wen model is not derived from first principles (24). Consequently, the values of its parameters are iteratively adjusted until the output force of the model closely aligns with experimental data. This model is characterized by its ability to capture the nonlinear and asymmetric behavior exhibited by MR dampers under varying operating conditions.

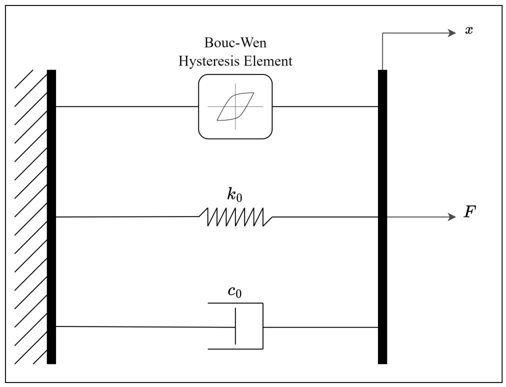

Figure 1: The Bouc-Wen model for identifying the dynamics of a MR damper, adapted from (24).

The remainder of this section will delve into the mathematical modeling of MR dampers using the Bouc-Wen parametric model, a widely recognized approach for capturing the nonlinear behavior of these devices (24). The characterization of the Bouc-Wen equation for the estimated damping force (F) of the MR damper as a function of damper displacement (x), velocity ($\dot{x}$), and prior state dependency (represented by z), is as follows:

$$F = \alpha z + c_0 \dot{x} + k_0 \left(x - x_0\right) \, , \tag{1}$$

where parameters α, c_0, k_0 are dependant upon applied voltages. Drawing from the prior research (24; 33), it is feasible to depict the relationship of these parameters with an effective voltage term u through linear expressions:

$$\alpha = \alpha_a + \alpha_b u \, , \tag{2}$$

$$c_0 = c_{0a} + c_{0b} u \, , \tag{3}$$

$$k_0 = k_{0a} + k_{0b} u \, . \tag{4}$$

The achievement of magnetorheological fluid rheological equilibrium necessitates the incorporation of a first-order filter applied to the voltage v for the efficient voltage u :

$$\dot{u} = \eta \left(u - v\right) \tag{5}$$

wherein η denotes a coefficient representing the adjustment rate. Variable z of Equation 1 denotes the hysteretic displacement, a fundamental component in quantifying the effects of the system's historical dependence on the resultant damping force. This hysteretic displacement may be modelled based on the following relation:

$$\dot{z} = -\gamma \left|\dot{x}\right| z \left|z\right|^{n-1} - \beta \left|\dot{x}\right| \left|z\right|^{n} + A\dot{x} \, , \tag{6}$$

where γ, β, A, and n are model parameters that exert control over the linearity during unloading and determine the smoothness of the transition from the pre-yield to the post-yield region, as demonstrated by Spencer and colleagues (24). Table 1 provides a summary, as well as a brief description of the functionality of parameters and variables employed in the Bouc-Wen model of hysteresis.

Table 1: Compiled model parameters for the Bouc-Wen model of hysteresis, with descriptions

Parameter	**Description**
α	Voltage dependant scaling factor
α_a	Shaping parameter for parameter α
α_b	Shaping parameter for parameter α
c_0	Voltage dependant viscous damping factor
c_{0a}	Shaping parameter for parameter c_0
c_{0b}	Shaping parameter for parameter c_0
k_0	Voltage dependant stiffness
k_{0a}	Shaping parameter for parameter k_0
k_{0b}	Shaping parameter for parameter k_0
γ	Hysteresis parameter controlling the shape and size of the hysteresis loop
β	Hysteresis parameter controlling the shape and size of the hysteresis loop
A	Hysteresis parameter controlling the shape and size of the hysteresis loop
η	Response time
n	Exponent parameter that determines the shape of the hysteresis loop
x_0	Initial deflection of accumulator
F	Damping force
x	Damper displacement
$\dot{x}$	Damper velocity
v	Applied voltage from power source
u	Efficient voltage

3. PHYSICS-INFORMED NEURAL NETWORKS

PINNs represent a recently popularized approach that combines NN with the known principles of physics, offering accurate predictions and insights into complex systems. This typically entails a specific implementation of physics-informed regularization, and enables the development of predictive models that not only make accurate predictions but also provide physical insights into the system's behavior. Regularization techniques have been fundamental in training ML models since their inception. Conventional regularization, such as Lasso (L1) or Ridge (L2) regularizations, incorporates an additional penalty term to reduce the model's capacity to overfit data that may not be reflective of the general behavior of the system, resulting in simpler and more robust solutions (1; 44). While regularization techniques have been used extensively, in the initial works on the topic of PINNs by Raissi and colleagues (16; 17), the authors aimed to leverage the structure of the physical system to learn more efficient representations. More specifically, the authors utilised the *a priori* information of various systems, effectively incorporating the governing equations of the physical system as regularizers within the loss function. This approach seeks to combine the advantages of physics-based models to enhance the accuracy, interpretability, and robustness of conventional data-driven solutions. Prior knowledge regarding the physical system is integrated as a part of the learning process, either as constraints or regularizers, effectively encoding the physical constraints to aid in guiding the optimization process in producing physically meaningful solutions (17).

Thus, PINNs presents an approach to leverage the power of NN to learn complex patterns and relationships from data, while also incorporating the underlying physical principles such as partial differential equations

(PDEs) or ordinary differential equations (ODEs) that govern the system (16; 17). Through the introduction of learning biases, PINNs significantly relaxes restrictions in terms of the quantity of data required to properly train deep learning algorithms (13; 45). PINNs are known for their ability to generate accurate predictions with small amounts of data, which is especially important in cases where data acquisition is expensive or challenging (12; 45; 46). These factors make PINNs particularly well-suited for applications in which the underlying physics of the system is well-understood.

The concept of leveraging the computational capabilities of NN for solutions to differential equations was initially presented by (47), however, its reach was limited due to limitations of computational power at the time. More recently, (17) popularized the concept through their study, where they demonstrated the effectiveness of PINNs in solving forward and inverse problems pertaining to governing differential equations of a physical system. The effectiveness of PINNs, as defined in the work of (17), is derived, in part, from their usage of the universal approximation capability of NN (48), which states that a neural network with a single-layered feed-forward network with an activation function may approximate any function, provided that it is comprised of a sufficient number of neurons. Naturally, researchers have extended this property to the solution of complex, non-linear differential equations, in which numerical or empirical solutions are difficult or impossible. In these scenarios, PINNs have been leveraged to learn the mapping between the input data and the output variables while enforcing the physical constraints of the system. In addition to their ability to incorporate prior knowledge, PINNs are capable of learning the solution to ODES or PDEs from incomplete data or data with noise, while simultaneously satisfying the governing equations of the system (17). Through this framework, researchers are able to build accurate models that provide insights into the underlying physical processes, making them a valuable tool in many scientific and engineering applications (49).

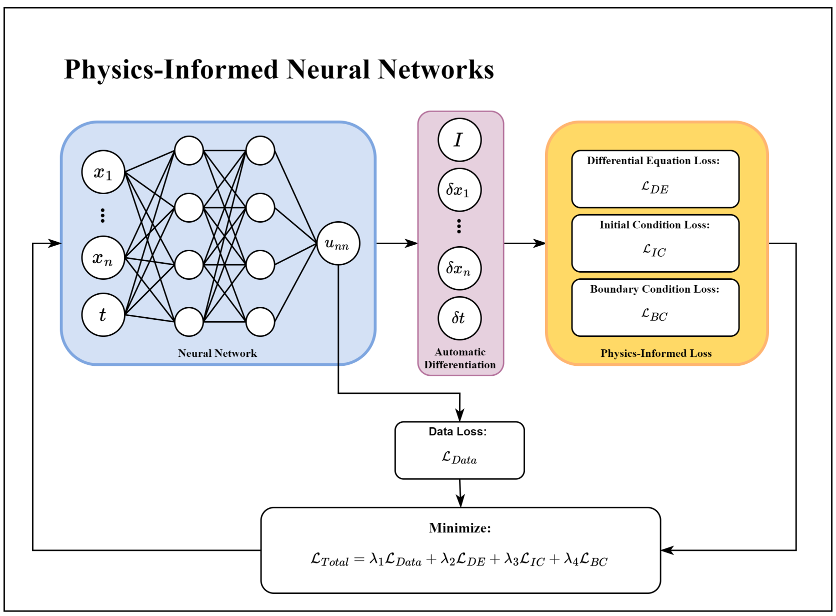

Figure 2: A representation of a physics-informed neural network, as initially proposed in (16).

The original PINN architecture by Rassi and colleagues (17), pictured in Figure 2 is based on the feed-forward structure, and employed to solve the first-order non-linear PDE. Various names exist for this structure in literature such as feed-forward neural networks, artificial neural networks, multi-layer perceptron neural networks, and deep neural detworks. The feed-forward neural network is a type of artificial neural network that consists of multiple layers of interconnected nodes, or neurons, that transmit information through weighted connections (1). In the context of PINNs, the input layer of the network corresponds to the physical domain, while the output layer represents the solution to the problem of interest. The intermediate layers, also known as hidden layers, provide the necessary computational power to map the input to the output.

4. INTEGRATION OF KNOWN PHYSICS WITH MACHINE LEARNING MODEL

The integration of the Bouc-Wen model for MR dampers within a PINN offers a promising avenue for advancing the study of structural and control systems engineering. This integration enables the development of a surrogate model for MR dampers capable of predicting resultant forces without necessitating explicit knowledge of Bouc-Wen model parameters or unobservable variables. This approach harnesses the universal approximative capabilities inherent in neural networks (48), providing a means to accurately estimate known functions associated with the Bouc-Wen model. Consequently, the surrogate model provides a practical and efficient method for simulating MR damper behavior in real-world applications. In this section, the equations governing the integration of the Bouc-Wen model within the physics-informed neural network will be detailed. These equations detail how the neural network effectively learns to approximate the complex behavior of MR dampers. Typically, employing the Bouc-Wen models for analysis would entail the tedious and time-consuming process of tuning the various mechanical parameters associated with the equations (42; 43). However, in this study, we propose a four-stage prediction process based on a hybrid physics-informed data-driven approach, inspired by prior works in the area (17; 50), that circumvents the need for explicit knowledge of model parameters by leveraging the power of neural networks.

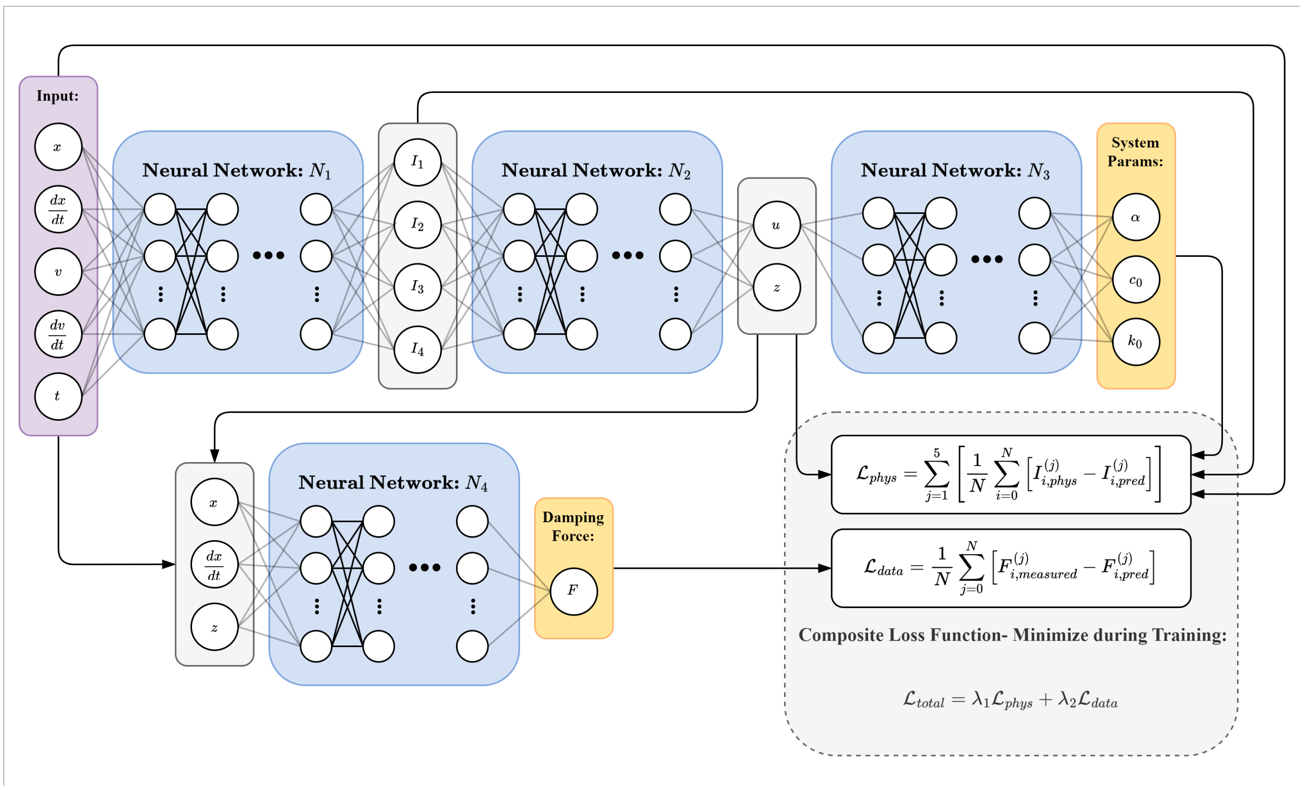

Figure 3: The overall workflow of the hybrid physics-informed data-driven neural network based surrogate model for modelling the dynamic and rheological behaviours of the MR damper.

The overall structure of the model is laid out as a cascaded architecture, comprised of four prediction stages, as illustrated in Figure 3. Utilising the universal approximation theorem, the neural network predicts the sequence of states for a given time interval. The initial stage employs a neural network to approximate derived states $\mathbf{I} = [I_1, I_2, I_3, I_4]^T$ from input data $\mathbf{D} = \left[x, \frac{dx}{dt}, v, \frac{dv}{dt}, t\right]^T$, given as:

$$\mathbf{I} = N_1(\mathbf{D}; \theta_1)\,, \tag{7}$$

where N_1 represents the network with its associated weights and biases θ_1. As values for u and z are not present in the input information, this estimate will not be optimal. Instead, this will be remedied by the training process, with a physics informed loss function. The derived states $\mathbf{I}$ may be derived through the application of numerical integration to components of the original Bouc-Wen equations independent of system parameters. The derivation of the states, based on the original Bouc-Wen equations are presented as follows. Integration is applied initially to equations 5 and 6:

$$\int_{t_0}^{t_i} \dot{z}\,(t)\,dt = -\gamma \int_{t_0}^{t_i} |\dot{x}(t)|\, z(t)\, |z(t)|^{n-1}\, dt - \beta \int_{t_0}^{t_i} \dot{x}(t)\, |z(t)|^{n}\, dt + A \int_{t_0}^{t_i} \dot{x}(t) dt\,, \tag{8}$$

$$\int_{t_0}^{t_i} \dot{u}(t) dt = \eta \int_{t_0}^{t_i} \left(u(t) - v(t)\right)\; dt\,. \tag{9}$$

The equations 8 and 9 may thus be expressed as a linear combination of derived states $\mathbf{I}$ and model parameters, which is also equivalent to the evolution of unobservable variables u and z over a specified time period of t_0 to t_i :

$$\int_{t_0}^{t_i} \dot{z}(t) dt = z(t_i) - z(t_0) = \gamma I_1(t) + \beta I_2(t) + A I_3(t)\,, \tag{10}$$

$$\int_{t_0}^{t_i} \dot{u}(t) dt = u(t_i) - u(t_0) = \eta I_4(t)\,, \tag{11}$$

where states $\mathbf{I}$ may be approximated numerically through the use of numerical integration methodologies. For the sake of simplicity, the trapezoid rule is employed in this study:

$$\begin{aligned}
I_1(t) &= -\int_{t_0}^{t_i} |\dot{x}(t)|\, z(t)\, |z(t)|^{n-1}\, dt \\
&= -\frac{1}{2} \sum_{i=0}^{i-1} \left[\left(|\dot{x}(t_i)|\, z(t_i)\, |z(t_i)|^{n-1} \right) + \left(|\dot{x}(t_{i+1})|\, z(t_{i+1})\, |z(t_{i+1})|^{n-1} \right) \right] (t_{i+1} - t_i)\ , \qquad (12)\\
I_2(t) &= -\int_{t_0}^{t_i} \dot{x}(t)\, |z(t)|^{n}\, dt \\
&= -\frac{1}{2} \sum_{i=0}^{i-1} \left[\left(\dot{x}(t_i)\, |z(t_i)|^{n} \right) + \left(\dot{x}(t_{i+1})\, |z(t_{i+1})|^{n} \right) \right] (t_{i+1} - t_i)\ , \qquad (13)\\
I_3(t) &= \int_{t_0}^{t_i} \dot{x}(t) dt = x\left(t_i\right) - x\left(t_0\right)\ , \qquad (14)\\
I_4(t) &= \int_{t_0}^{t_i} u(t) - v(t)\ dt = \frac{1}{2} \sum_{i=0}^{i-1} \left[u(t_i) - v(t_i) + \left(u(t_{i+1}) - v(t_{i+1}) \right) \right] (t_{i+1} - t_i)\ . \qquad (15)
\end{aligned}$$

The subsequent network employs the predicted states to predict the rate of change in efficient voltage u, and hysteretic displacement z. This process enforces that the network N_2 models the explicit relation defined in equations 9 and 10:

$$\left[\Delta u, \Delta z\right]^{T} = N_2\left(\mathbf{I}; \theta_2\right)\ . \tag{16}$$

From the above representation of the rate of change for efficient voltage and hysteretic displacement, given an initial value, it is possible to obtain the values for both variables: $[u, z]^{T}$ at each instance in time. Given that knowledge of the efficient voltage is now available, a neural network is employed to approximate equations 2 to 4. For a given input of efficient voltage, the model parameters varying with applied voltage may be estimated via:

$$[\alpha, c_0, k_0]^T = N_3\left(u; \theta_3\right) , \tag{17}$$

where the estimated parameters are to be used in re-constructing the original equation, to be employed as a loss function by which the overall cascaded network is to be penalized by. Finally, the model employs neural network N_4 to provide force predictions, based on initial inputs, and predicted values for hysteretic displacement. This, again, models the explicit relation discussed in 1.

$$F = N_4\left(\left[x, \frac{dx}{dt}, z\right]^T ; \theta_3\right) . \tag{18}$$

The cascaded networks are trained concurrently utilising a composite loss function that penalizes the deviations from known physics, as well as deviations from training data. The loss is comprised of a physics-based and data-based component, where the physics-based loss is primarily enforcing the continuity of developed states **I** through time. The physics-based loss depends on the reconstruction of each of the four states developed, utilising predicted values. Comparison is also made between the reconstruction of equation 1 based on intermediate components from the cascaded network:

$$\mathcal{L}_{phys}^{(1)} = I_1(t) - \frac{1}{2}\sum_{i=0}^{i-1}\left[\left(\left|\dot{x}(t_i)\right| z(t_i) \left|z(t_i)\right|^{n-1}\right) + \left(\left|\dot{x}(t_{i+1})\right| z(t_{i+1}) \left|z(t_{i+1})\right|^{n-1}\right)\right](t_{i+1} - t_i) , \tag{19}$$

$$\mathcal{L}_{phys}^{(2)} = I_2(t) - \frac{1}{2}\sum_{i=0}^{i-1}\left[\left(\dot{x}(t_i) \left|z(t_i)\right|^{n}\right) + \left(\dot{x}(t_{i+1}) \left|z(t_{i+1})\right|^{n}\right)\right](t_{i+1} - t_i) , \tag{20}$$

$$\mathcal{L}_{phys}^{(3)} = I_3(t) - \left(x\left(t_i\right) - x\left(t_0\right)\right) , \tag{21}$$

$$\mathcal{L}_{phys}^{(4)} = I_4(t) - \frac{1}{2}\sum_{i=0}^{i-1}\left[u(t_i) - v(t_i) + \left(u(t_{i+1}) - v(t_{i+1})\right)\right](t_{i+1} - t_i) , \tag{22}$$

$$\mathcal{L}_{phys}^{(5)} = \frac{1}{N}\sum_{i=1}^{N}\left(F_{measured,i} - \left(\alpha_i z_i + c_{0,i}\dot{x} + k_{0,i}(x_i + x_0)\right)\right)^2 . \tag{23}$$

where N represents the sequence length of the input fed through the neural network at one time, not to be confused with aforementioned denotations of neural networks N_1 to N_4. The total physics-based loss is thus the sum of prior physics-based loss components:

$$\mathcal{L}_{phys} = \sum_{j=1}^{5}\left[\frac{1}{N}\sum_{i=1}^{N}\left(\mathcal{L}_{phys,i}^{(j)}\right)^2\right] . \tag{24}$$

The data-driven component of the loss is derived based on the resultant predicted force by network N_4, which is compared against the measured force from the experimental setup, depicted in equation 25.

$$\mathcal{L}_{data} = \frac{1}{N}\sum_{i=1}^{N}\left(F_{measured,i} - F_{predicted,\ i}\right)^2 . \tag{25}$$

The overall loss for training the network is presented as a composite of individual physics-based and data-driven losses, featuring a weighted sum of each component:

$$\mathcal{L}_{total} = \lambda_1 \mathcal{L}_{phys} + \lambda_2 \mathcal{L}_{data} \,. \tag{26}$$

where parameters λ_1 and λ_2 represent the weights assigned to each loss component. Depending on their assigned value, the resultant network may be tuned to learn more so from the physical model or from data. In the subsequent section, the resultant predictions of the surrogate model is presented. The efficacy of the PINN surrogate model is scrutinized via comparisons with empirical data. Specifically, the model's proficiency in replicating the damper's force-displacement-velocity characteristics across various operation scenarios, as well as various combinations of component weight during training are explored.

5. RESULTS AND DISCUSSION

In this section, the results of utilising a PINN to serve as a surrogate model for a MR damper are presented. The primary objective of this study is to leverage the *a priori* knowledge of the system's physical behavior, as described by the Bouc-Wen equations, to enhance the predictive capability of the neural network model. The performance of the PINN surrogate model is evaluated through comparisons with experimental data. Specifically, the effectiveness of the PINN in reproducing the damper's force-displacement-velocity characteristics under various operating conditions is assessed. Furthermore, the ability of the PINN to capture the dynamic response of the MR damper to excitation inputs, as well as performance in various training scenarios are investigated.

The data analyzed in this study was collected from a physical experimental setup featuring an MR damper, illustrated in Figure 4. This setup provides practical insights into the performance of MR dampers under controlled conditions. Core to its function is the MR damper itself, the damping properties of which may be varied through voltage control via the programmable power supply. Force measurements are obtained through the resistive load cell. The overall motion of the assembly is actuated by a linear actuator. To facilitate data collection, a program on the main computer collects the data collected from various aforementioned components, and writes said data to a SQL database.

As previously stated, the model was trained in a hybrid manner, incorporating a composite loss function to effectively balance the physics-based loss derived from the Bouc-Wen model's differential equations and the conventional data-driven loss associated with force data from experiments. A range of scenarios was explored to identify an optimal equilibrium between physics-informed and data-driven methodologies. Models were trained utilising the listed weights below. An 80-20 split was employed to isolate the training and validation datasets, and the model was tested on a never before seen dataset. Table 2 outlines the various cases and results for combinations of weights for the composite loss function of the model evaluated on the validation dataset. Models are evaluated based on Root Mean Squared Error (RMSE) of predictions.

Table 2: Weights and corresponding error on predictions for the surrogate model developed.

Physics-based weight λ_1	Data-driven weight λ_2	Ratio	RMSE $[N]$
1	1	1	10.75
0.1	0.5	0.2	8.87
0.1	1	0.1	9.76
0.1	10	0.01	7.85
0.5	0.1	5	9.97
0.5	1	0.5	8.52
0.5	10	0.05	7.09
1	0.1	10	11.54
1	0.5	2	8.19
10	0.1	100	11.65
10	0.5	20	13.34

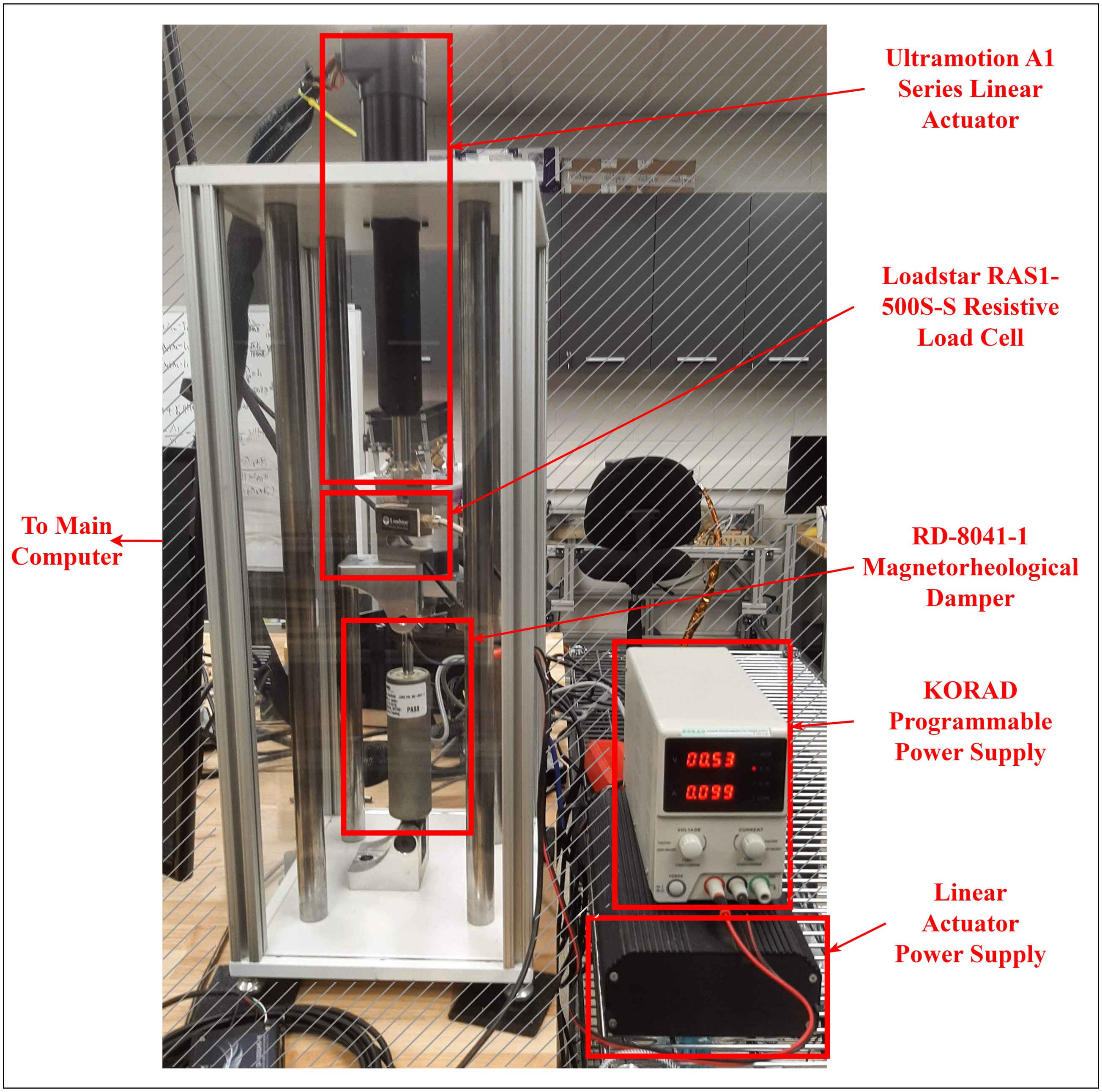

Figure 4: The experimental setup utilised for data collection.

In general, it was observed that assigning a higher weight to the data-driven component relative to the physics-based component yielded superior performance. This observation can be attributed to the inherent limitations and imperfections of the Bouc-Wen model, which serves as the foundation for the physics-based loss. As the physics-based component becomes more dominant, it increasingly imposes constraints based on the assumptions and simplifications inherent in the Bouc-Wen model, potentially leading to inaccuracies in capturing the system's true behavior. Conversely, a higher weight assigned to the data-driven component allows the model to adapt more effectively to the complexities and deviations present in the experimental setup or the device itself. By prioritizing the data-driven aspect, the model becomes more adept at capturing and accommodating any discrepancies between the idealized physics and the real-world observations. Furthermore, in scenarios where noise is prevalent, a higher data weight becomes particularly advantageous. The presence of noise can significantly disrupt the calculation of the physics-based loss function, leading to erratic behavior and diminished performance. In contrast, the data-driven component is more resilient to noise, enabling the model to better discern patterns and trends amidst the fluctuations, thereby enhancing its overall predictive capability. Thus, the preference for a higher data weight in such cases is justified not only by its ability to attenuate to the system's characteristics but also by its resilience to noise-induced perturbations, ultimately contributing to improved model performance and accuracy in predicting the damping force of MR dampers.

The efficacy of different weighting compositions is illustrated through the presentation of subsequent figures showcasing notable combinations. These figures will include plots depicting force over time, force-displacement relationships, and force-velocity profiles. The data presented in the plots are presented with 52 mV and 2.63 V applied voltage to the MR damper itself, and represent a sample from experiments conducted. These samples depict the extremes of the voltage range tested. They serve as illustrative points to demonstrate the behavior of the MR damper under varying voltage conditions, encompassing a spectrum of its response. In analyzing the results, it is evident that the more physics-based weighting did not capture the unique hysteretic profile in force-velocity plots, as illustrated in 5 and 6. The force-displacement and force-time relationship also deviates relatively significantly from the actual measured behavior of the MR damper.

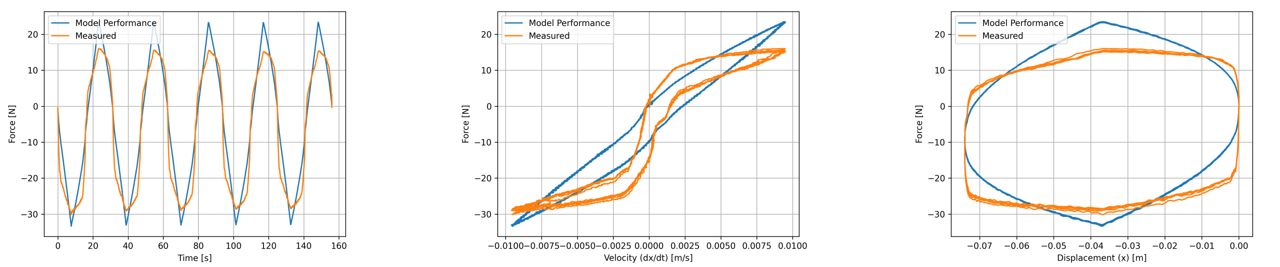

(a) (b) (c)

Figure 5: Sample results (a) Force-time plots, (b) Force-velocity plots, and (c) Force-displacement plots for model performance on test dataset with applied voltage of 524 mV. Measurements constant acceleration oscillation along entire stroke length. PINN-based surrogate model trained with $\lambda_1 = 10$, and $\lambda_2 = 0.1$.

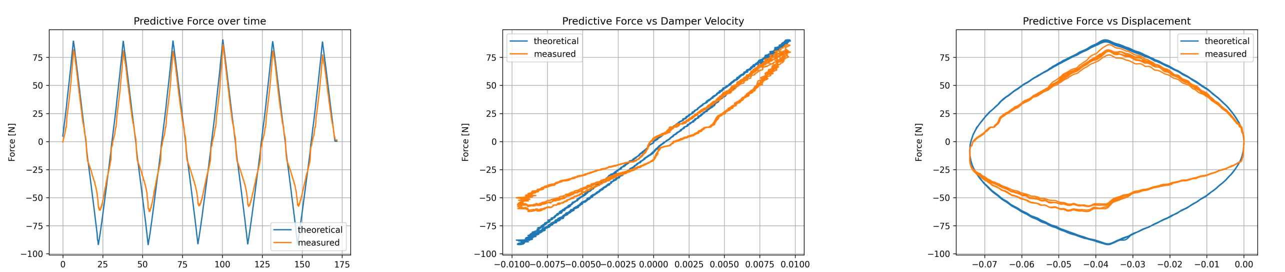

(a) (b) (c)

Figure 6: Sample results (a) Force-time plots, (b) Force-velocity plots, and (c) Force-displacement plots for model performance on test dataset with applied voltage of 2.63 V. Measurements constant acceleration oscillation along entire stroke length. PINN-based surrogate model trained with $\lambda_1 = 10$, and $\lambda_2 = 0.1$.

On the other hand, the combination of $\lambda_1 = 0.5$ and $\lambda_2 = 10$ shows significant improvement in terms of minimizing discrepancies in the form of error, but there is still clear room for enhancement. The behavior of the MR damper is not exactly captured here either, suggesting that further refinement of the weighting parameters is necessary for better model performance. The performance are illustrated in 7 and 8.

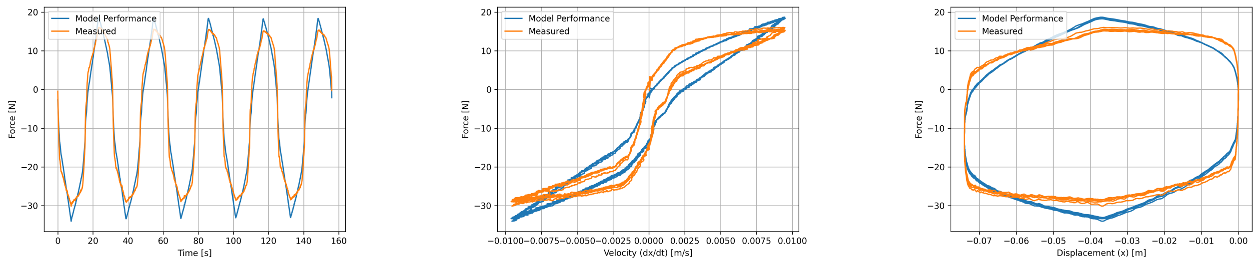

(a) (b) (c)

Figure 7: Sample results (a) Force-time plots, (b) Force-velocity plots, and (c) Force-displacement plots for model performance on test dataset with applied voltage of 524 mV. Measurements constant acceleration oscillation along entire stroke length. PINN-based surrogate model trained with $\lambda_1 = 0.5$, and $\lambda_2 = 10$.

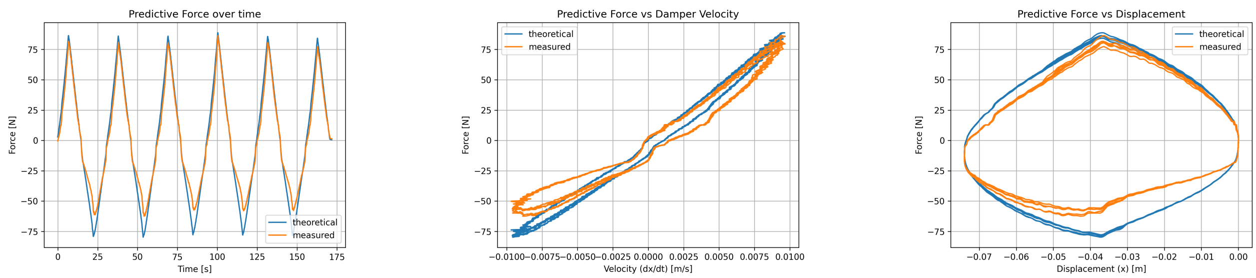

(a) (b) (c)

Figure 8: Sample results (a) Force-time plots, (b) Force-velocity plots, and (c) Force-displacement plots for model performance on test dataset with applied voltage of 2.63 V. Measurements constant acceleration oscillation along entire stroke length. PINN-based surrogate model trained with $\lambda_1 = 0.5$, and $\lambda_2 = 10$.

Depending on the relative weighting of the physics-based and data-driven loss components within the composite loss function, varying levels of accuracy were observed. Notably, assigning a higher weight to the physics-based component resulted in a model behavior more closely resembling that of numerical simulations. However, this approach revealed limitations in capturing the dynamics of the roll-off region, characteristic of the Bouc-Wen model upon which the physics-based loss is based. In particular, the force-velocity hysteresis phenomena in this region were found to be misrepresented, indicating areas for further refinement. Conversely, optimizing for higher accuracy often favored a greater emphasis on the data-driven loss component. While this led to improved performance on the test dataset, questions arise regarding the robustness of the model across a broader range of operating conditions. Under such circumstances, the surrogate model tended to exhibit characteristics more aligned with a conventional black-box ML approach, potentially raising concerns about overfitting to the specific dataset. This highlights the need for thorough validation and generalizability testing to ensure the model's applicability to unseen scenarios.

The improved computational efficiency of the PINN-based surrogate model compared to traditional numerical simulations should also be noted. The PINN framework allows for rapid predictions of the damper's behavior, which is advantageous for real-time applications and large-scale studies. To quantify this advantage, a comparison was made between the computational times required for numerical simulation and PINN prediction. For a dataset of approximately 100,000 data points, the process of identifying Bouc-Wen model parameters and simulating outputs through numerical methods took an average of 1 minute, 2 seconds, and 35 milliseconds. In contrast, the PINN-based surrogate model, without hardware acceleration, achieved the same predictions in approximately 0.756 seconds with a single pass of the neural network. This reduction in computational time highlights the practicality and efficiency of the PINN approach, especially in scenarios requiring rapid analysis and decision-making.

5.1 Limitations

Despite the promising capabilities demonstrated by the PINN, several constraints must be acknowledged to provide a comprehensive understanding of its applicability and potential shortcomings. Firstly, it is important to note that the training of the PINN still relies, to a lesser extent than traditional neural networks, on the availability of data points. Due to practical constraints and experimental limitations, the dataset used for training may not fully encompass the entire range of operating conditions and configurations encountered in real-world scenarios. Consequently, the predictive accuracy of the PINN model may be compromised, particularly in regions of the parameter space with sparse data coverage.

Moreover, while the incorporation of physics-based constraints through the Bouc-Wen equations enhances the model's interpretability and robustness, it also introduces certain limitations. The Bouc-Wen model, while widely used to describe the nonlinear behavior of MR dampers, is inherently an approximation and may not fully capture all aspects of the damper's response. Specifically, the model may struggle to accurately represent the behavior of MR dampers in certain operating regimes, such as high voltage excitation or extreme displacement conditions. This limitation arises from the simplified nature of the Bouc-Wen equations, which may not adequately account for complex phenomena such as magnetic saturation or hysteresis effects observed in MR dampers.

Furthermore, the composite loss function employed in training the PINN, which combines physics-based constraints and data fidelity terms, may lead to a trade-off between accuracy and robustness. While the inclusion of physics-based constraints helps enforce physical consistency, it may also restrict the flexibility of the model, particularly in regions of the parameter space where the physics-based constraints are less accurate or reliable. As a result, the PINN model may exhibit reduced accuracy or predictive performance in certain scenarios, necessitating careful consideration of its limitations and potential areas for improvement in future research endeavors.

5.2 Future Work

In future work, employing neural networks specialized for time series analysis, such as Recurrent Neural Networks (RNNs), Gated Recurrent Units (GRUs), or Long Short-Term Memory (LSTM) networks, holds promise for enhancing the modeling capabilities of the surrogate model. Given the temporal nature of the data generated by the MR damper system, these architectures offer the potential to capture intricate dynamics and temporal dependencies more effectively. Expanding the scope of the study to encompass various other models of the MR damper, such as the modified Bouc-Wen model proposed by Spencer and colleagues, presents an avenue for refining the accuracy of the surrogate model. While this model offers improved fidelity in capturing the hysteretic behavior, its increased complexity necessitates careful consideration of computational resources and modeling trade-offs. Incorporating advanced hyperparameter optimization schemes can further enhance the performance of the neural network model by effectively balancing the influence of physics-based constraints and data-driven learning objectives. Employing techniques tailored to optimize network hyperparameters efficiently, such as Bayesian optimization or evolutionary algorithms, may facilitate the discovery of optimal configurations in a more time-effective manner compared to conventional grid or random search methods. Extending the application of the developed surrogate model to real-time condition monitoring represents a promising avenue for practical implementation. By leveraging the capabilities of PINNs, the model can be deployed for continuous monitoring and assessment of MR damper performance, enabling proactive maintenance strategies, and enhancing system reliability and efficiency.

6. CONCLUSION

This study explores the utilisation of PINNs for surrogate modeling of MR dampers, aiming to predict their dynamic behavior accurately under various operational conditions. The incorporation of the Bouc-Wen hysteresis model into the training process of cascaded neural networks facilitates the development of a surrogate model that balances computational efficiency with accuracy. Through experimentation, it was observed that different weighting compositions between the physics-based and data-driven loss components influence the model's performance. Assigning a higher weight to the data-driven component generally resulted in improved predictive capability, especially in scenarios with prevalent noise. However, emphasizing the physics-based component led to a model behavior more aligned with numerical simulations but exhibited limitations in capturing certain dynamics, particularly in the roll-off region characteristic of the Bouc-Wen model. Further refinement of weighting parameters is necessary to enhance model performance, ensuring a better representation of the MR damper's behavior across a broader range of operating conditions. Additionally, thorough validation and generalizability testing are imperative to assess the model's applicability to unseen scenarios and prevent overfitting to specific datasets.

References

[1] Murphy, K. P., [*Machine learning: a probabilistic perspective*], MIT press (2012).

[2] LeCun, Y., Bengio, Y., and Hinton, G., "Deep learning," *nature* **521**(7553), 436–444 (2015).

[3] Goodfellow, I., Bengio, Y., and Courville, A., [*Deep learning*], MIT press (2016).

[4] Hilal, W., Gadsden, S. A., and Yawney, J., "A machine learning-based state estimation approach for varying noise distributions," in [*Signal Processing, Sensor/Information Fusion, and Target Recognition XXXII*], **12547**, 47–55, SPIE (2023).

[5] Li, Y., "Research and application of deep learning in image recognition," in [*2022 IEEE 2nd international conference on power, electronics and computer applications (ICPECA)*], 994–999, IEEE (2022).

[6] Traore, B. B., Kamsu-Foguem, B., and Tangara, F., "Deep convolution neural network for image recognition," *Ecological informatics* **48**, 257–268 (2018).

[7] Shafiq, M. and Gu, Z., "Deep residual learning for image recognition: A survey," *Applied Sciences* **12**(18), 8972 (2022).

[8] Young, T., Hazarika, D., Poria, S., and Cambria, E., "Recent trends in deep learning based natural language processing," *ieee Computational intelligenCe magazine* **13**(3), 55–75 (2018).

[9] Deng, L. and Liu, Y., [*Deep learning in natural language processing*], Springer (2018).

[10] Diligenti, M., Roychowdhury, S., and Gori, M., "Integrating prior knowledge into deep learning," in [*2017 16th IEEE international conference on machine learning and applications (ICMLA)*], 920–923, IEEE (2017).

[11] Surucu, O., Gadsden, S. A., and Yawney, J., "Condition monitoring using machine learning: A review of theory, applications, and recent advances," *Expert Systems with Applications* **221**, 119738 (2023).

[12] Zheng, B., Li, T., Qi, H., Gao, L., Liu, X., and Yuan, L., "Physics-informed machine learning model for computational fracture of quasi-brittle materials without labelled data," *International Journal of Mechanical Sciences* **223**, 107282 (2022).

[13] Cuomo, S., Di Cola, V. S., Giampaolo, F., Rozza, G., Raissi, M., and Piccialli, F., "Scientific machine learning through physics–informed neural networks: Where we are and what's next," *Journal of Scientific Computing* **92**(3), 88 (2022).

[14] Fu, J., Xiao, D., Fu, R., Li, C., Zhu, C., Arcucci, R., and Navon, I. M., "Physics-data combined machine learning for parametric reduced-order modelling of nonlinear dynamical systems in small-data regimes," *Computer Methods in Applied Mechanics and Engineering* **404**, 115771 (2023).

[15] Sun, Y., Sengupta, U., and Juniper, M., "Physics-informed deep learning for simultaneous surrogate modelling and pde-constrained optimization," *Bulletin of the American Physical Society* **67** (2022).

[16] Raissi, M., Perdikaris, P., and Karniadakis, G. E., "Physics informed deep learning (part i): Data-driven solutions of nonlinear partial differential equations," *arXiv preprint arXiv:1711.10561* (2017).

[17] Raissi, M., Perdikaris, P., and Karniadakis, G. E., "Physics-informed neural networks: A deep learning framework for solving forward and inverse problems involving nonlinear partial differential equations," *Journal of Computational physics* **378**, 686–707 (2019).

[18] Zhao, Y., Jiang, C., Vega, M. A., Todd, M. D., and Hu, Z., "Surrogate modeling of nonlinear dynamic systems: a comparative study," *Journal of Computing and Information Science in Engineering* **23**(1), 011001 (2023).

[19] Haghighat, E., Raissi, M., Moure, A., Gomez, H., and Juanes, R., "A physics-informed deep learning framework for inversion and surrogate modeling in solid mechanics," *Computer Methods in Applied Mechanics and Engineering* **379**, 113741 (2021).

[20] Sun, Y., Sengupta, U., and Juniper, M., "Physics-informed deep learning for simultaneous surrogate modeling and pde-constrained optimization of an airfoil geometry," *Computer Methods in Applied Mechanics and Engineering* **411**, 116042 (2023).

[21] Eghbalian, M., Pouragha, M., and Wan, R., "A physics-informed deep neural network for surrogate modeling in classical elasto-plasticity," *Computers and Geotechnics* **159**, 105472 (2023).

[22] Sun, L., Gao, H., Pan, S., and Wang, J.-X., "Surrogate modeling for fluid flows based on physics-constrained deep learning without simulation data," *Computer Methods in Applied Mechanics and Engineering* **361**, 112732 (2020).

[23] Yang, G., Spencer Jr, B., Carlson, J., and Sain, M., "Large-scale mr fluid dampers: modeling and dynamic performance considerations," *Engineering structures* **24**(3), 309–323 (2002).

[24] Spencer Jr, B., Dyke, S., Sain, M., and Carlson, J., "Phenomenological model for magnetorheological dampers," *Journal of engineering mechanics* **123**(3), 230–238 (1997).

[25] Alizadeh, R., Allen, J. K., and Mistree, F., "Managing computational complexity using surrogate models: a critical review," *Research in Engineering Design* **31**(3), 275–298 (2020).

[26] Yao, G., Yap, F., Chen, G., Li, W., and Yeo, S., "Mr damper and its application for semi-active control of vehicle suspension system," *Mechatronics* **12**(7), 963–973 (2002).

[27] Desai, R. M., Jamadar, M. E. H., Kumar, H., Joladarashi, S., Rajasekaran, S., and Amarnath, G., "Evaluation of a commercial mr damper for application in semi-active suspension," *SN Applied Sciences* **1**, 1–10 (2019).

[28] Seong, M.-S., Choi, S.-B., and Sung, K.-G., "Control strategies for vehicle suspension system featuring magnetorheological (mr) damper," *Vibration Analysis and Control: New Trends and Developments; InTech: London, UK* , 97–114 (2011).

[29] Nguyen, Q.-H. and Choi, S.-B., "Optimal design of mr shock absorber and application to vehicle suspension," *Smart materials and Structures* **18**(3), 035012 (2009).

[30] Yang, G., Spencer Jr, B. F., Jung, H.-J., and Carlson, J. D., "Dynamic modeling of large-scale magnetorheological damper systems for civil engineering applications," *Journal of Engineering Mechanics* **130**(9), 1107–1114 (2004).

[31] Jung, H.-J., Spencer Jr, B., Ni, Y., and Lee, I., "State-of-the-art of semiactive control systems using mr fluid dampers in civil engineering applications," *Structural Engineering and Mechanics* **17**(3-4), 493–526 (2004).

[32] Cho, S.-W., Jung, H.-J., and Lee, I.-W., "Smart passive system based on magnetorheological damper," *Smart Materials and Structures* **14**(4), 707 (2005).

[33] Talatahari, S., Kaveh, A., and Mohajer Rahbari, N., "Parameter identification of bouc-wen model for mr fluid dampers using adaptive charged system search optimization," *Journal of mechanical science and technology* **26**, 2523–2534 (2012).

[34] Maharani, E. T., Ubaidillah, U., Imaduddin, F., Wibowo, W., Utami, D., and Mazlan, S. A., "A mathematical modelling and experimental study of annular-radial type magnetorheological damper," *International Journal of Applied Electromagnetics and Mechanics* **66**(4), 543–560 (2021).

[35] Lee, A. S., Wu, Y., Gadsden, S. A., and AlShabi, M., "Interacting multiple model estimators for fault detection in a magnetorheological damper," *Sensors* **24**(1), 251 (2023).

[36] Soltane, S., Montassar, S., Ben Mekki, O., and El Fatmi, R., "A hysteretic bingham model for mr dampers to control cable vibrations," *Journal of Mechanics of Materials and Structures* **10**(2), 195–206 (2015).

[37] Kamath, G. M. and Werely, N. M., "Nonlinear viscoelastic-plastic mechanisms-based model of an electrorheological damper," *Journal of Guidance, Control, and Dynamics* **20**(6), 1125–1132 (1997).

[38] Hong, S., Choi, S., Choi, Y. T., and Wereley, N. M., "A hydro-mechanical model for hysteretic damping force prediction of er damper: experimental verification," *Journal of Sound and Vibration* **285**(4-5), 1180–1188 (2005).

[39] Zhang, W. and Xu, Y. L., "Vibration analysis of two buildings linked by maxwell model-defined fluid dampers," *Journal of sound and vibration* **233**(5), 775–796 (2000).

[40] El Majdoub, K., Giri, F., and Chaoui, F.-Z., "Backstepping adaptive control of quarter-vehicle semi-active suspension with dahl mr damper model," *IFAC Proceedings Volumes* **46**(11), 558–563 (2013).

[41] Jiménez, R. and Álvarez-Icaza, L., "Lugre friction model for a magnetorheological damper," *Structural Control and Health Monitoring* **12**(1), 91–116 (2005).

[42] Zhu, H., Rui, X., Yang, F., Zhu, W., and Wei, M., "An efficient parameters identification method of normalized bouc-wen model for mr damper," *Journal of Sound and Vibration* **448**, 146–158 (2019).

[43] Negash, B. A., You, W., Lee, J., and Lee, K., "Parameter identification of bouc-wen model for magnetorheological (mr) fluid damper by a novel genetic algorithm," *Advances in Mechanical Engineering* **12**(8), 1687814020950546 (2020).

[44] Alsadi, N., Hilal, W., Surucu, O., Giuliano, A., Gadsden, S. A., Yawney, J., and AlShabi, M. A., "Neural network training loss optimization utilizing the sliding innovation filter," in [*Artificial Intelligence and Machine Learning for Multi-Domain Operations Applications IV*], **12113**, 577–589, SPIE (2022).

[45] Wu, Y., Sicard, B., and Gadsden, S. A., "A review of physics-informed machine learning methods with applications to condition monitoring and anomaly detection," *arXiv preprint arXiv:2401.11860* (2024).

[46] Xu, S., Sun, Z., Huang, R., Guo, D., Yang, G., and Ju, S., "A practical approach to flow field reconstruction with sparse or incomplete data through physics informed neural network," *Acta Mechanica Sinica* **39**(3), 322302 (2023).

[47] Lagaris, I. E., Likas, A., and Fotiadis, D. I., "Artificial neural networks for solving ordinary and partial differential equations," *IEEE transactions on neural networks* **9**(5), 987–1000 (1998).

[48] Hornik, K., Stinchcombe, M., and White, H., "Multilayer feedforward networks are universal approximators," *Neural networks* **2**(5), 359–366 (1989).

[49] Raymond, S. J. and Camarillo, D. B., "Applying physics-based loss functions to neural networks for improved generalizability in mechanics problems," *arXiv preprint arXiv:2105.00075* (2021).

[50] Hu, Y., Guo, W., Long, Y., Li, S., et al., "Physics-informed deep neural networks for simulating s-shaped steel dampers," *Computers & Structures* **267**, 106798 (2022).